



Synthesis of Gold Nanoparticles Using Schiff Base Derivative of Ceftriaxone Sodium With Isatin as A Reducing and Stabilizing Agent

AHLAM JAMEEL ABDULGHANI* and SAJA KHALIL MOHUEE

University of Baghdad, Department of Chemistry, College of Science, Jaderiya, Baghdad, Iraq.

*Corresponding author E-mail: almumaraj@gmail.com

<http://dx.doi.org/10.13005/ojc/330327>

(Received: March 31, 2017; Accepted: April 29, 2017)

ABSTRACT

Gold nanoparticles AuNPs were synthesized in aqueous solutions at different conditions via the reduction of sodium tetrachloroaurate (III) (NaAuCl_4) by the Schiff base ligand sodium (6S)-7-((Z)-2- (methoxyimino)-2-(2-((Z)-2- oxoindolin-3- ylideneamino) thiazol-4-yl) acetamido)-3-((2-methyl-6- oxido-5-oxo-2,5-dihydro-1,2,4-triazin-3-ylthio) methyl)-8-oxo-5-thia-1-azabicyclo[4.2.0]oct-2-ene-2-carboxylate (ISCR) derived from the condensation reaction of ceftriaxone sodium (CR) with 1H-indole-2,3-dione (isatin, Is). The synthesized AuNPs were characterized by UV- visible spectroscopy, FTIR spectroscopy, X-ray diffraction (XRD), scanning electron microscope (SEM), and atomic force microscope (AFM).

Key word: Ceftriaxone, Isatin , Schiff base, AuNPs, surface plasmon bands

INTRODUCTION

The synthesis of AuNPs via the reduction of AuCl_4^- in aqueous solution by using the antibiotic ceftriaxone (CR) has been reported earlier¹. 1H-indole-2,3-dione (isatin, Is) and its Schiff base with β - lactam antibiotic cefotaxime were also reported as reducing and stabilizing agents in the synthesis of AuNPs^{2, 3}. The sizes, shapes and stability of the prepared AuNPs were found to change with type of ligand, reactant concentrations, pH and reaction temperature. The condensation of isatin

with cefotaxime was found to decrease the rate of reduction of Au(III) ions compared with the free isatin molecules^{2,3}. In this work the reduction of AuCl_4^- to AuNP in aqueous solution is investigated at different conditions ,using the Schiff base ligand sodium (6S)-7-((Z)-2-(methoxyimino)-2-(2-((Z)-2-oxoindolin-3- ylideneamino) thiazol-4-yl) acetamido) -3-((2-methyl-6- oxido-5-oxo-2,5-dihydro-1,2,4-triazin-3-ylthio) methyl)-8-oxo-5- thia-1-azabicyclo[4.2.0]oct-2-ene-2-carboxylate(ISCR)(Fig. 1) that has been previously prepared from the condensation reaction of ceftriaxone antibiotic(CR) with isatin⁴

MATERIALS AND METHODS

Materials

Ceftriaxone sodium ($C_{18}H_{16}N_8O_7S_3Na_2 \cdot 3.5H_2O$) (LDP), isatin (Aldrich), sodium tetrachloroaurate (III) dihydrate ($NaAuCl_4 \cdot 2H_2O$) (BDH), were used as received from suppliers. Buffer solutions of different pH were prepared from potassium dihydrogen orthophosphate KH_2PO_4 99% (Fluka), dipotassium hydrogen orthophosphate, K_2HPO_4 , 99%, (Fluka) and phosphoric acid H_3PO_4 (Analar, BDH). The synthesis and characterization of the the Schiff base ligand ISCR has been reported earlier⁴

Instrumentation

Electronic spectra of the prepared AuNPs solutions were obtained on a (200–1100 nm) SHIMADZU 1800 Double Beam UV-Visible spectrophotometer. The binding of Schiff base ligand to AuNPs was analyzed by FTIR spectra using

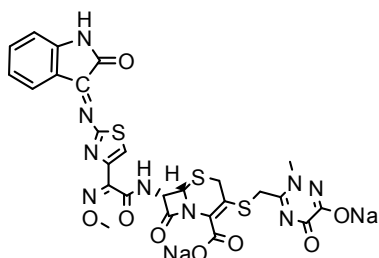


Fig. 1: Structure of Schiff base Ligand ISCR

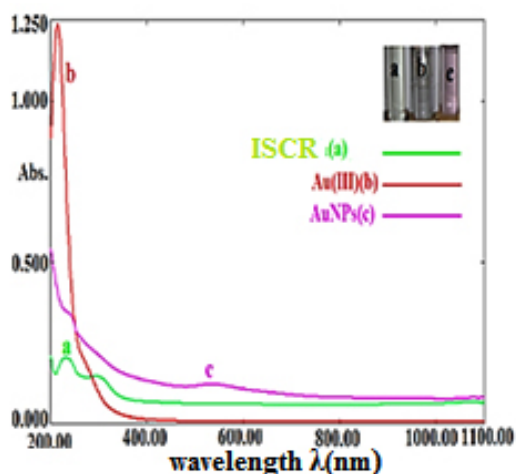


Fig. 2: The uv-visible spectra of a- ISCR(1.266×10^{-4} M), b- $AuCl_4^-$ (2.514×10^{-4} M) and c-synthesized AuNPs in aqueous solutions after 24 h

a SHIMADZU FT-IR 8400 S spectrophotometer. Size and morphology of AuNPs were determined by Scanning electron microscope (SEM) and by atomic force microscopy AFM images using SEM (KYKY-EM3200) and AFM model AA 3000 SPM 220 V-Angstrom (Advanced INC. USA) respectively. XRD analyses were measured by using a SHIMADZU XRD-6000 x-ray diffractometer with a Cu-K α ($\lambda = 0.154060$ nm) radiation source.

Synthesis of AuNPs at different conditions

An aqueous solution of the Schiff base ligand ISCR ($Na_2C_{26}H_{19}N_9O_8S_3 \cdot 2H_2O \cdot 1.5CH_3OH$) (1.266×10^{-4} M) was prepared by dissolving 0.1027 g of the ligand in 1000 ml deionized water (DDW). A stock aqueous solution of $AuCl_4^-$ (2.514×10^{-3} M) was prepared by dissolving 0.1 g of $NaAuCl_4 \cdot 2H_2O$ in 100 ml distilled deionized water (DDW) in 100 ml volumetric flask. A standard solution of $AuCl_4^-$ (2.514×10^{-4} M) was prepared by diluting 10 ml of the stock solution to 100 ml. Ten aqueous solutions containing a constant concentration of $NaAuCl_4 \cdot 2H_2O$ solution (7.542×10^{-5} M) and different concentrations of ISCR (6.33×10^{-6} , 1.266×10^{-5} , 1.899×10^{-5} , 2.532×10^{-5} , 3.165×10^{-5} , 3.798×10^{-5} , 5.064×10^{-5} , 6.33×10^{-5} , 7.596×10^{-5} and 8.862×10^{-5} M) were prepared by adding 0.25, 0.5, 0.75, 1.0, 1.25, 1.5, 2, 2.5, 3, 3.5 ml of a freshly prepared solution of ISCR (1.266×10^{-4} M) to 1.5 ml of $AuCl_4^-$ solution (2.514×10^{-4} M) followed by dilution to 5 ml. The concentration ratios of ISCR / $AuCl_4^- = 0.084$, 0.168, 0.252, 0.336, 0.42, 0.504, 0.671, 0.84, 1.007 and 1.175 respectively. The uv-visible spectra of the prepared solutions were measured at room temperature to obtain the optimum concentration ratio of ISCR / $AuCl_4^-$. The effect of temperature on the synthesis rate of AuNPs was studied spectrophotometrically by heating ten (5 ml) solutions of the selected concentration ratio of ISCR / $AuCl_4^-$ for 5 minutes at 35, 40, 45, 50, 55, 60, 65, 70, 75 and 80 °C respectively and at selected temperature for different heating times (5, 10, 15, 20, 25, 30, 35, 40, 45 and 60 min) in a water bath. The pH effect on AuNPs synthesis was also studied spectrophotometrically, using the selected ISCR / $AuCl_4^-$ ratio at pH media: 2.37, 3.25, 4.15, 5.70, 6.30, 7.22, 8.38, 8.83, 10.14 and 11.16.

RESULTS AND DISCUSSION

UV-Vis spectrophotometry

Concentration effect

Fig.2 shows the uv-visible spectra of Schiff base ligand, ISCR(a), AuCl₄⁻ (b) and AuNPs

solution prepared from mixing 1.5 mL of ISCR (1.266×10⁻⁴ M) with 0.75 mL of AuCl₄⁻ (2.514×10⁻⁴ M) diluted to 5 mL(c). The spectrum of ISCR displayed two bands at λ 230 and 297 nm attributed to π→π* transition as was reported earlier⁴, while the spectrum of AuCl₄⁻ solution corresponds to

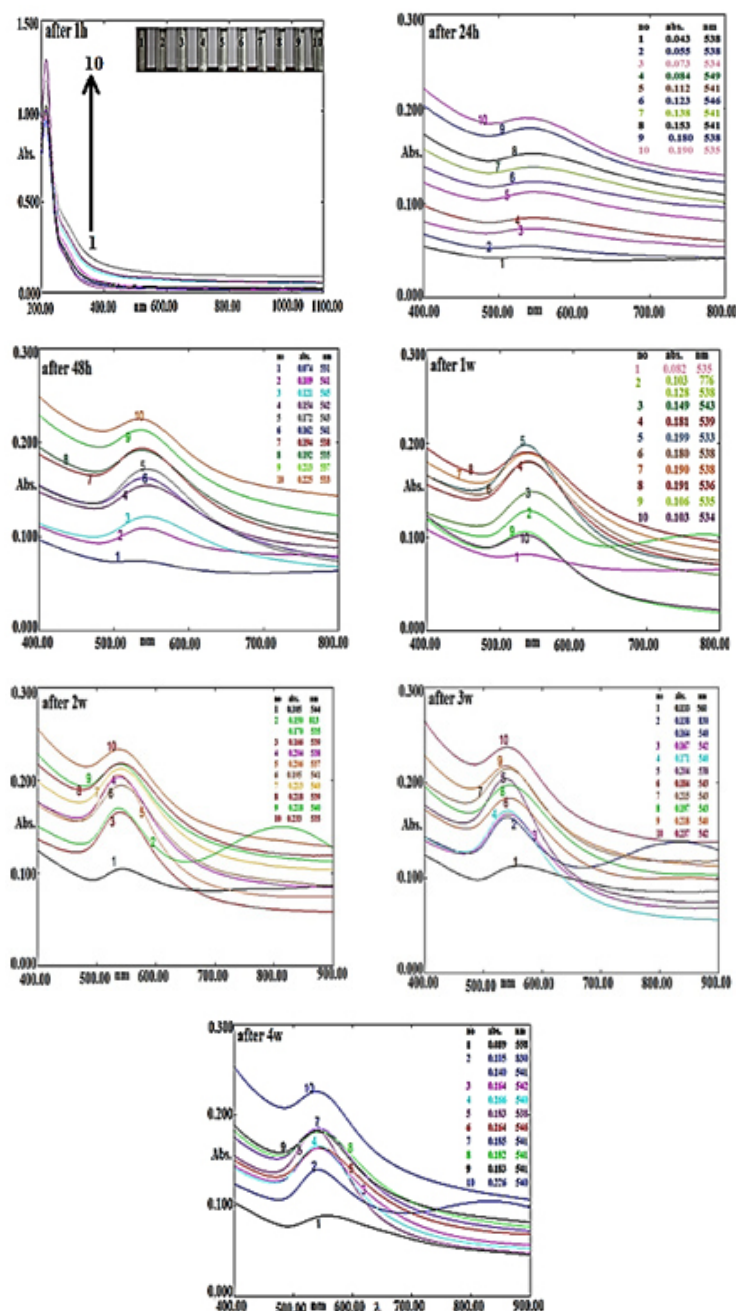


Fig. 3: Absorption spectra of ISCR-synthesized AuNPs at different concentration ratios of ISCR/AuCl₄⁻(0.084, 0.168, 0.252, 0.336, 0.42, 0.504, 0.671, 0.84, 1.007 and 1.175(1-10 respectively))

square planar tetrachloroaurate complex^{5,6}. After 24h of preparation, the solution mixture developed a pink color with absorption maxima at 533 nm assigned to the surface plasmon band SPB of spherical AuNPs⁷⁻¹³. This indicates that Au(III) ions have been reduced by Schiff base ligand to form AuNPs.

Fig.3 shows the variation in the absorption spectra of AuNPs solutions prepared from a constant concentration of AuCl_4^- (3.771×10^{-5} M) and different concentrations of ISCR (6.33×10^{-6} , 1.266×10^{-5} , 1.899×10^{-5} , 2.532×10^{-5} , 3.165×10^{-5} , 3.798×10^{-5} , 5.064×10^{-5} , 6.33×10^{-5} , 7.596×10^{-5} and 8.862×10^{-5} M). (1-10 respectively). No color change and no SPB were detected in all solutions until 24 h when the spectra gave increased absorption of single bands at $\lambda = (538, 538, 534, 549, 541, 546, 541, 541, 538$ and 535 nm respectively assigned to SPR of spherical AuNPs⁷⁻¹². After 48 h the spectra of all solutions showed increased absorptions with the bands of solutions 1,4,6-10 being shifted to lower wavelengths and appeared at $\lambda = (531, 542, 541, 538, 535, 537$ and 533 nm respectively). Absorption bands of solutions 2, 3 and 5 were shifted to higher wavelengths and appeared at $\lambda = 541, 545, 543$ nm respectively, referring to larger size or aggregation of AuNPs. After one week, solution 2 exhibited

two high absorption bands appeared at 538 and 776 nm which may be attributed to the formation of non-spherical AuNPs^{5, 14-17}. After three weeks, band absorptions increased and their positions were shifted to higher wavelengths and appeared at $\lambda = 560, (540$ and $830), 540, 542, 540, 538, 543, 543, 540$ and 542 nm respectively. After four weeks the intensity of SPBs decreased. The best performance was recorded by solutions 9 and 10 (ISCR/ AuCl_4^- 1.007 and 1.175 respectively) the spectra of which exhibited higher SPB absorbance and higher stability with time compared with the other solutions. This result is quite different from those reported on using ceftriaxone (CR) and isatin (Is) separately when optimum concentration ratios of CR/ AuCl_4^- and Is/ AuCl_4^- were $(0.172)^1$ and $(9.52)^2$ respectively which reflects the effect of different ligand structures on gold nanoparticle synthesis.

Temperature effect

Fig.4 shows the spectra of ten solutions of ISCR / AuCl_4^- (1.007) after being heated at 35-80°C for 5 minutes. All solutions exhibited weak absorption bands appeared at $\lambda = 549, 550, 540, 536, 539, 535, 529, 534, 531$ and 525 nm respectively, assigned to the SPB of spherical AuNPs with estimated size range about 10-60 nm^{7,9,10,13}. The reaction time to form

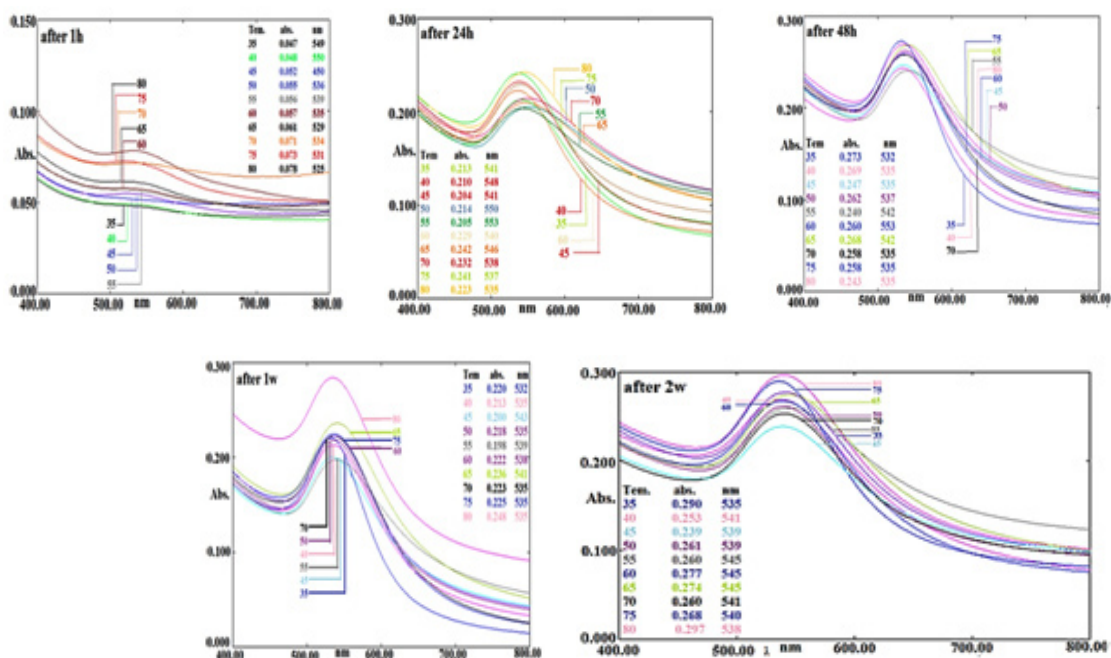


Fig.4: Absorption spectra with time for AuNPs synthesized from a solution of ISCR/ AuCl_4^- 1.007 heated at 35° -80°C

AuNPs was reduced with increasing temperatures and all solutions exhibited continuous increase in absorbance of SPBs for more than 48h. As in the case of CR¹, the highest rate of AuNPs synthesis was recorded at 80 °C which remained stable for more than two weeks .Fig. 5 shows the spectra of AuNPs in ten solutions of the concentration ratio ISCR /AuCl₄:(1.007) heated at 80°C for 5 min to 60 min. The spectra of all solutions exhibited single absorption bands in the visible region appeared at

$\lambda = (524, 529, 538, 530, 528, 541, 534, 534, 530$ and 533 nm respectively. After 24h the bands of solutions heated at 5, 25, 40, 45 and 60 min. were shifted to higher wavelengths and appeared at (530, 531, 538, 533 and 534 nm respectively), while those of the solutions heated for 15,30 and 35 min were shifted to lower wavelength and appeared at $\lambda = (531, 537$ and 519 nm respectively). The spectra of all solutions showed increased absorption of SPB with time for one week, followed by decreased absorption after

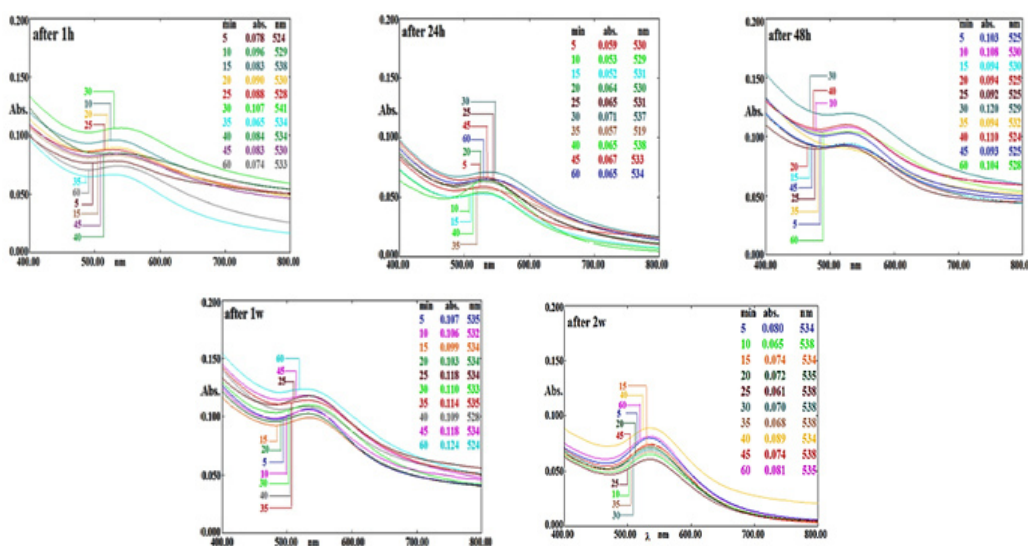


Fig. 5: Absorption spectra of AuNPs prepared from a solution of ISCR/ AuCl₄ (1.007) heated at 80°C for different time intervals (5-60 min)

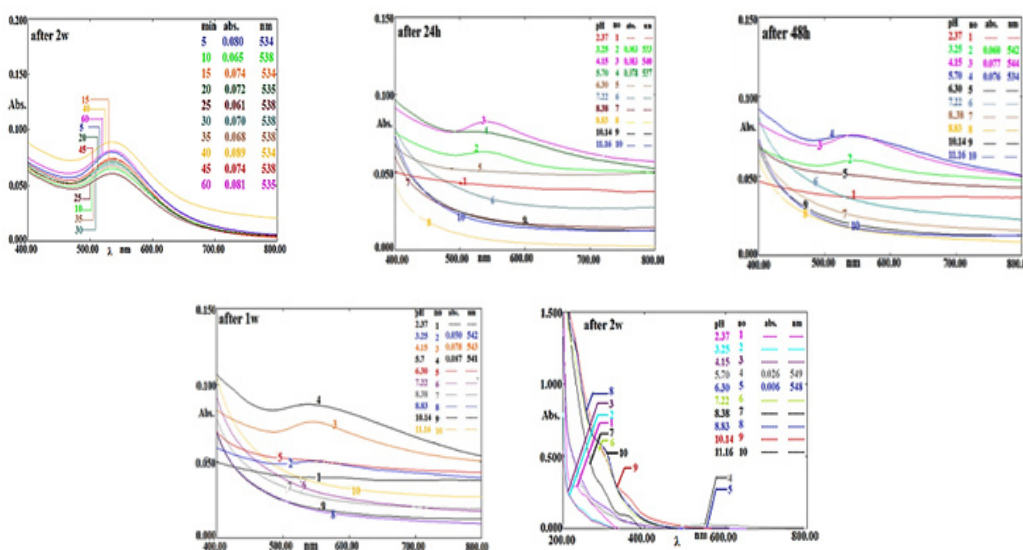


Fig. 6: Absorption spectra of AuNPs synthesized at different pH values

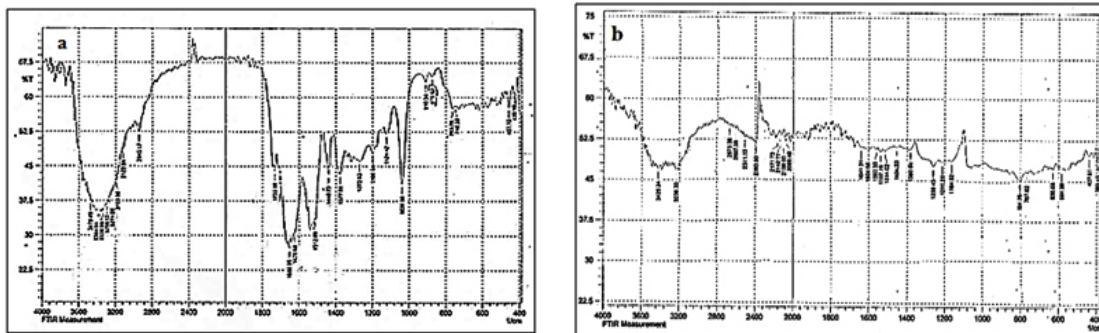


Fig. 7: FT-IR spectrum of a- ISCR and b- ISCR-synthesized AuNPs

two weeks. The best heating times were 5 and 30 minutes. However, the reduction process by ISCR was of lower rate compared with that of free CR and isatin^{1,2} which may be attributed to the removal of free amino group of CR moiety and the change in redox behavior of isatin moiety .

pH Effect

Fig.6 shows the absorption spectra of ISCR- synthesized AuNPs solutions at different pH media (2.37, 3.25, 4.15, 5.70, 6.30, 7.22, 8.38, 8.83, 10.14 and 11.16, 1-10 respectively) using ISCR/AuCl₄⁻ concentration ratio (1.007).

After 1h of preparation no color change and no SPB were detected in all solutions. After 24h only the solutions (2,3 and 4) of pH (3.25-5.70) gave pink colors and their spectra exhibited a single weak absorption band at λ 533, 540 and 537 nm respectively. The best performance was exhibited at pH=5.7 and to less extent at pH=4.15 as the two solutions remained stable for two weeks. Despite the difference in ligand /AuCl₄⁻ ratio, the performances of ISCR were almost similar to those of CR and Is at nearly the same pH values^{1,2}. The low rate of reduction of Au(III) in highly acidic solutions may be attributed to the protonation of functional groups responsible for electron donation while neutral and basic solutions may result in the formation of stable Au(III) hydroxyl anion complexes such as [AuCl₃(OH)]⁻, [AuCl₂(OH)₂]⁻, [AuCl(OH)₃]⁻ or [Au(OH)₄]⁻^{18,19}. The reduction process by ISCR was also of lower rate compared with that of CR and isatin^{1,2}.

Characterization of AuNPs FTIR spectra

The infrared band assignment of the FTIR spectrum of ISCR shown in Fig. 7a was reported

earlier⁴. The spectrum of ISCR- synthesized AuNPs (Fig. 7b) shows that the positions of the bands attributed to azomethine (-HC=N-)(1625.88 cm⁻¹) , ν C=O of lactam(1733.89 cm⁻¹), ν C=O overlapped amide and ester(1660.10 cm⁻¹), ν_{asy} (COO⁻) and ν_{sy} (COO⁻) (1640.25 and 1430.15 cm⁻¹ respectively) of the free ligand were shifted and appeared at 1604, 1680, 1641.31 and (1646 and 1434) cm⁻¹ respectively. The two bands observed at 3425.34 and 3236.33 cm⁻¹ in Fig.7b may be assigned to N-H stretching vibration of NH₂ group resulted from the oxidation of isatin moiety which led to ring opening². These data refer to the binding of AuNPs with functional groups of the Schiff base ligand.

X-Ray Diffraction (XRD)

Fig. 8 shows the diffraction pattern of AuNPs prepared from aqueous solution of ISCR/ AuCl₄⁻ = (1.007). Four diffraction peaks were observed at 2θ = (38.2522, 44.4910, 64.6450 and 77.919) degrees corresponding to the planes (111), (200), (220) and (311) of face centered cubic lattice structure of AuNPs^{9,20} which are in agreement with the XRD pattern data available in the JCPDS file no.(04-0784).The crystalline sizes of the nanoparticle were estimated using unmodified Scherrer's equation^{21,22}. The average size was found 38.5 nm corresponding to the planes (111) and (200), and 80 nm according to the planes (111), (200), (220) and (311).

Scanning Electron Microscopy (SEM)

The SEM image of AuNPs at room temperature and at heating temperature range 35-80 °C for 5 min. showed particles of regular spherical shapes with a wide size distribution ranging between 44-97 nm and average size of 73 nm (Fig. 9). However, heating the aqueous solution

at 80 °C for 30 minutes gave rise to different shapes and sizes of AuNPs which appeared as spherical, nanorods and irregular shapes as is shown in Fig.10. The average diameter of nanosphers was 43.39 nm, while average diameter and length of nanorods were 43 and 178 nm respectively. This result shows that the heating period at 80°C affects the size and morphology of AuNPs in this study.

Atomic Force Microscopy (AFM)

Fig.11 shows the AFM micrographs of the ISCR- synthesized AuNPs at heating temperature 80 °C for 5 minutes which have spherical shapes with average diameter of 82.28 nm. The AFM image of the same solution heated at 80 °C for 30 minutes (Fig.12) showed the presence of different sizes and shapes of AuNPs with average particle sizes 85.52 nm.

Antibacterial activity

The antibacterial activity of ISCR and ISCR-capped AuNPs have been tested against the pathogenic bacteria gram negative *Escherichia coli*, and gram positive *Pseudomonas aeruginosa*, *Staphylococcus aureus* and *Streptococcus pneumonia* compared with the activity of CR and CR-capped AuNPs that has been reported earlier¹, using drop diffusion method. The diameter of inhibition zones caused by each test sample was measured in (mm) and the results are described in Table 1. The ISCR-capped AuNPs showed the highest activity against all bacterial cultures compared with CR, ISCR and CR- capped AuNPs. These results indicate that AuNPs enhanced the activity of Schiff base ligand especially against *Pseudomonas Aeruginosa* and *Staphylococcus aureus*. The *Escherichia coli* was more sensitive to the four tested solutions compared with the other three cultures.

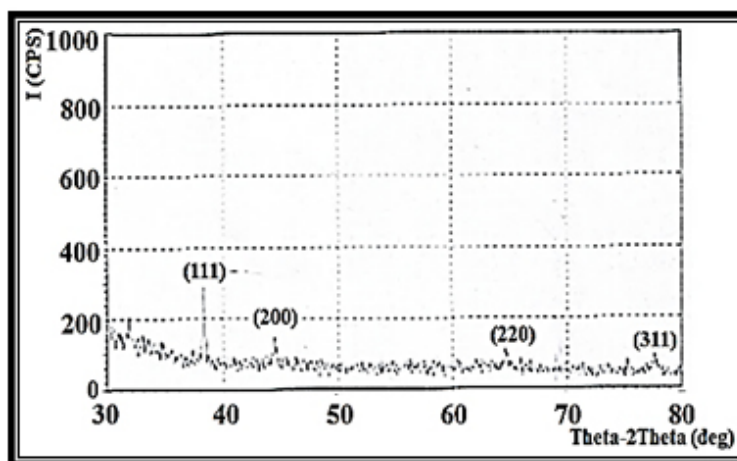


Fig. 8: XRD pattern of ISCR-conjugated AuNPs

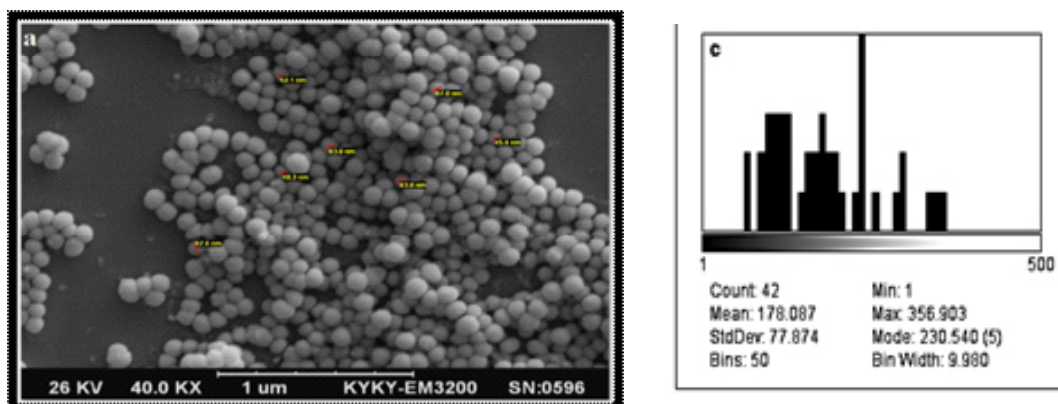


Fig. 9: a-SEM b-particle size distribution of ISCR- synthesized AuNPs heated at 80°C for 5min

Table 1: Inhibition zones (mm) exhibited by CR, ISCR and their conjugated AuNPs against some pathogenic bacteria

Sample	Inhibition zone (mm)			
	<i>Escherichia Coli</i>	<i>Pseudomonas Aeruginosa</i>	<i>Staphylococcus aureus</i>	<i>Streptococcus Pneumonia</i>
CR[1]	17.5	-	1	-
CR-capped AuNPs[1]	20	-	1	1
ISCR	20	-	-	3
ISCR-capped AuNPs	25	7.5	10	5

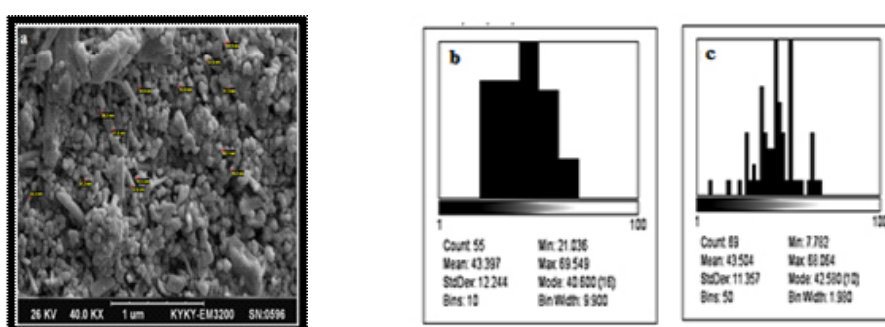


Fig. 10:a-SEM and particle size distribution of spherical (b) and rod like(c) ISCR-synthesized AuNPs heated at 80°C for 30 min

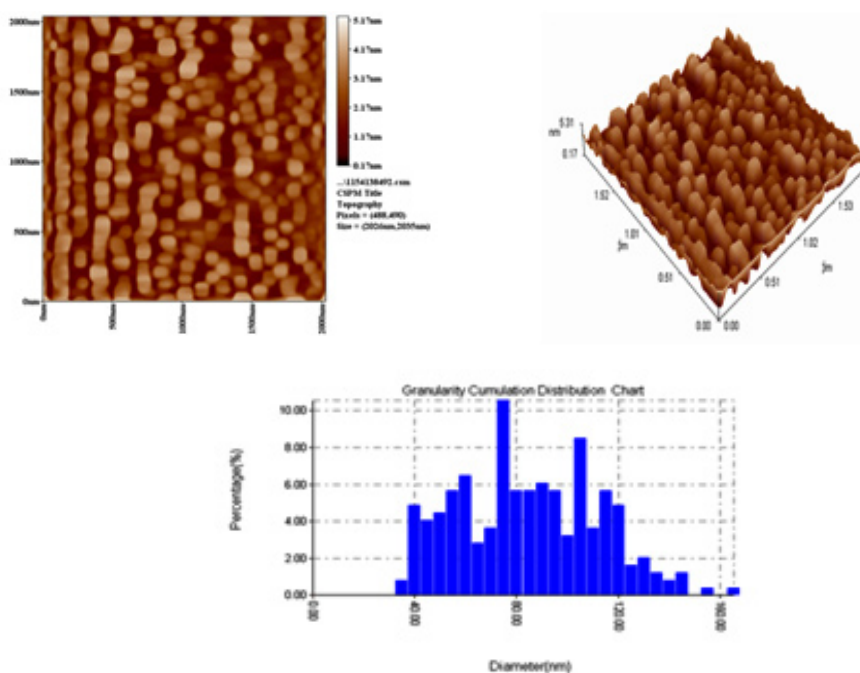


Fig.11: AFM pictures and size distribution of ISCR-synthesized AuNPs heated at 80°C for 5 min. Average diameter 82.28 nm.

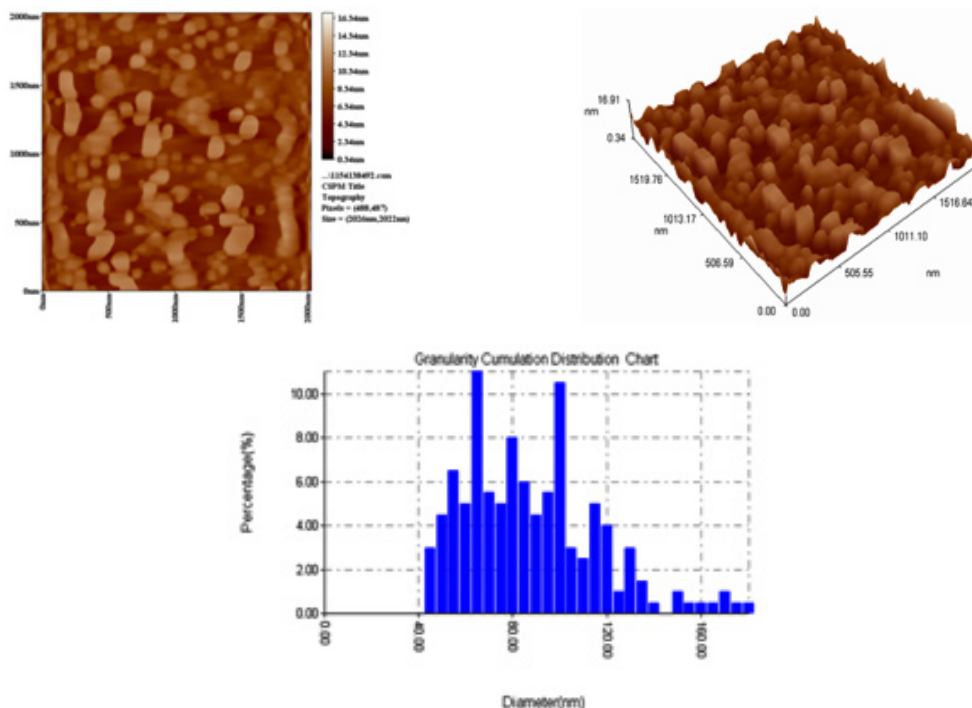


Fig.12:AFM pictures and size distribution of ISCR-synthesized AuNPs heated at 80°C for 30 min. Average diameter 85.52 nm

CONCLUSIONS

AuNPs conjugates were successfully synthesized from the reduction of Au(III) ions with the Schiff base derivative of ceftriaxone antibiotic with isatin (ISCR) at different concentration ratio of ISCR /AuCl₄⁻, temperature and pH media. The particles were characterized by uv-visible spectroscopy and XRD analysis, and their conjugation with ISCR functional groups was proved by FTIR spectroscopy. The optimum conditions for AuNPs synthesis were

ISCR /AuCl₄⁻ 1.007, pH 5.7, at 80 °C. Heating at 80 °C for 30 minutes changed the morphology of synthesized AuNPs from totally regular spherical shapes to a mixture of spherical, nanorods and irregular shapes. The condensation of amino group with the carbonyl group of isatin was found to decrease the rate of AuNPs synthesis compared with the performance of the two free separate molecules. Conjugation of ISCR with AuNPs enhanced its antibacterial activity.

REFERENCES

1. Abdulghani, A. J.; Mohuee, S. K. *Iraqi Journal of Science*. **2015**, *56*(3C), 2425-2438..
2. Abdulghani A. J.; Hussain, R. K. *Baghdad Science Journal*. **2014**, *11*(3), 1201-1216)
3. Abdulghani, A. J.; Hussain, R. K. *Journal of Chemical, Biological and Physical Sciences, Section A, Chemical Sciences*. **2015**, *5*(4), 3668-3684.
4. Abdulghani, A. J.; Mohuee, S. K. *Journal of Chemical, Biological and Physical Sciences, Section A*. **2016**, *6*(2), 579-595.
5. Link, S.; El-Sayed, M. A. *The Journal of Physical Chemistry*, **1999**, *103*, 4212-4217.
6. Jiang, G.; Wang, L.; Chen, W. *Materials Letters*, **2007**, *61*, 278–283.
7. Bhattacharya, D.; Saha, B.; Mukherjee, A.; Santra, C.R.; Karmakar, P. *Nanoscience and Nanotechnology*, **2012**, *2*(2), 14-21.
8. Zhang, L.; Swift, J.; Butts, C. A.; Yerubandi, V.; Dmochowski, I. J. *Journal of Inorganic*

- Biochemistry*, **2007**, *101*, 1719–1729.
9. Rai, A.; Prabhune, A.; Perry, C. C. *Journal of Materials Chemistry*, **2010**, *20*, 6789–6798.
 10. Demurtas, M.; Perry, C. C. *Gold Bull.*, **2013**, *47*(2014), 103–107.
 11. Brown, A.; Smith, K.; Samuels, T. A.; Lu, J.; Obare, S.; Scott, M. E. *Applied and Environmental Microbiology*, **2012**, *78*(8), 2768–2774.
 12. Qian, L.; Sha, Y.; Yang, X. *Thin Solid Films*, **2006**, *515*, 1349–1353.
 13. Jayalakshmi, K.; Ibrahim, M.; Rao, K. V. *International Journal of Electronic and Electrical Engineering*, **2014**, *7*(2), 159-164.
 14. Boopathi, S.; Senthilkumar, S.; Phani, K. L. *Journal of Analytical Methods in Chemistry*, **2012**, *212*, Article ID 348965, Doi:10.1155/2012/348965, 6 pages.
 15. Johan, M. R.; Chong, L. C.; Hamizi, N. A. *International Journal of Electrochemical Science*, **2012**, *7*, 4567-4573.
 16. Singh, P. P.; Bhakat, C. *Chemistry and Materials Research*, **2012**, *2*(1), 82-87.
 17. Shi, W.; Casas, J.; Venkataramasubramani, M.; Tang, L. *International Scholarly Research Network ISRN Nanomaterials*, **2012**, ID 659043, doi:10.5402/2012/659043, 9 pages.
 18. Young, J. K.; Lewnski, N. L.; Langsner, R. J.; Kennedy, L. C.; Satyanarayan, A.; Nammalvar, V.; Lin, A. Y.; Drezek, R. A. *Nanoscale Research Letters*, **2011**, *6*(421), 11 pages.
 19. Majziki, A.; Fulop, L.; Scapo, E.; Bogar, F.; Martinek, T.; Penke, B.; Biro, G.; Dekany, I. *Colloids Surf. B: Biointerfaces*, **2010**, *81*, 235-241.
 20. Zhang, Y.; Wei, S.; Chen, S., *International Journal of electrochemical science*, **2013**, *8*, 6493 – 6501.
 21. Monshi, A.; Foroughi, M. R.; Monshi, M. R. *World Journal of Nano Science and Engineering*, **2012**, *2*, 154-160.
 22. Firdhouse, M. J.; Lalitha, P.; Sripathi, S. K. *Digest Journal of Nanomaterials and Biostructures*, **2014**, *9*(1), 385-393